Coordinating dynamic traffic-power systems under decentralized, centralized, and information-sharing decision environments

Hongping Wang, Adam Abdin, Yi-Ping Fang, Jakob Puchinger, Enrico Zio

Coordinating dynamic traffic-power systems under decentralized, centralized, and information-sharing decision environments

Hongping Wang[a], Adam F.Abdin[a], Yi-Ping Fang[a,*], Jakob Puchinger[a], Enrico Zio[b,c]

[a] *Université Paris-Saclay, CentraleSupélec, Laboratoire Génie Industriel, 3 rue Joliot-Curie, Gif-sur-Yvette, France.*
[b] *Energy Department, Politecnico di Milano, 20156 Milano, Italy.*
[c] *Mines ParisTech, PSL Research University, CRC, Sophia Antipolis, France.*

Abstract

This paper proposes a dynamic traffic-electric power network model to investigate the interdependent electric power and road transport systems, whose operations are linked via the local marginal electricity price and the electric vehicles (EVs) charging demand. For the electric road network (ERN), a novel formulation based on the link transmission model is proposed to: 1) accommodate the critical features of EVs and fast charging stations (FCSs), such as EV with different driving ranges, initial states of charge of EVs, number of chargers and their charging power in a FCS; 2) explicitly model the charging process of EVs; 3) solve the optimal dynamic traffic assignment problem considering the mix of EVs and gasoline vehicles. For the economic operation of the power distribution network (PDN), an alternating current optimal power flow model is solved to minimize the electricity expenditure. Moreover, we propose mathematical algorithms to model the decentralized, centralized and information-sharing decision-making environments, so that the operational difference and social benefits of coordinating traffic-power systems can be compared. The proposed models and algorithms are applied to an illustrative traffic-power system. The results show that the decentralized decision-making always results in losses of operational cost and renewable integration, compared to the centralized decision making; however, these losses

*Corresponding author, Email address: yiping.fang@centralesupelec.fr

can be greatly mitigated by having ERN and PDN operators share information about the planned EV charging demand and the projected locational marginal electricity price.

Keywords: Traffic-power system, Electric vehicles, Charging stations, Coordination, Decision-making environments, Link transmission model

---

[1] Nomenclature

Indices

a	index of links
t	index of periods
s	index of destinations
c	index for classes of EVs
e	index for energy levels of EVs

The electrified road network sets

$\mathcal{A}$	set of arcs
$\mathcal{N}$	set of nodes
$A(i)$ $(B(i))$	set of links whose tail (head) node is i
$\mathcal{A}_R$	set of source arcs
$\mathcal{A}_S$	set of sink arcs
$\mathcal{A}_G$	set of general arcs
$\mathcal{A}_C$	set of charging arcs
$\mathcal{T}$	set of periods

Parameters

[1]*Corresponding author: Email address: yiping.fang@centralesupelec.fr

ϕ	time value
p_a^{ev}	charging power of charging link a
$NC_a(t)$	number of chargers at charging link a during period t
δ	period length
L_a	physical length of link a
$k_{jam}/q_{max}/v_f$	jam density/ maximum flow/ free-flow speed
w	backward shock-wave speed, $w = q_{max} \cdot v_f/(q_{max} - k_{jam} \cdot v_f)$
α_a^t	average charging speed for charging link a during period t, $\alpha_a^t = p_a^{ev}/(\eta \cdot v_f)$
$If_a(t)$	inflow capacity of link a during period t
$Of_a(t)$	outflow capacity of link a during period t
$DG_a^s(t)$	cumulative gasoline vehicle travel demand between the entry of origin link a and destination s at the end of period t
ν_a	free-flow travel time on link a, $\nu_a = L_a/(\delta \cdot v_f)$
β_a	travel time required by the backward shock wave from the exit to the entry of link a, $\beta_a = L_a/(\delta \cdot w)$

Variables

$U_a(t)$	cumulative number of vehicles that enter link a by the end of period t
$V_a(t)$	cumulative number of vehicles that leave link a by the end of period t
$UG_a(t)$	cumulative number of GVs that enter link a by the end of interval t
$UG_a^s(t)$	cumulative number of GVs that enter link a to destination s by the end of period t

$VG_a(t)$ cumulative number of GVs that leave link a by the end of interval t

$VG_a^s(t)$ cumulative number of GVs that leave link a to destination s by the end of period t

$UE_{a,c}^{s,e}(t)$ cumulative number of EVs of class c with energy level e that enter link a to destination s by the end of period t

$VE_{a,c}^{s,e}(t)$ cumulative number of EVs of class c with energy level e that leave link a to destination s by the end of period t

$x_{a,c}^{s,e}(t)$ occupancy of EVs of class c with energy level e at charging link a during period t

$\hat{x}_{a,c}^{s,e}(t)$ occupancy of EVs of class c with the **updated** energy level e at charging link a during period t

The electric vehicle sets

$\mathcal{C}$ set of electric vehicle classes

Parameters

B_c battery capacity of EVs of class c

E_c maximum energy level of the EVs of class c

η energy consumption of EVs

ρ_a energy levels required to traverse link a, $\rho_a = L_a/\eta$

L_c^{max} driving range of EVs of class c, $L_c^{max} = B_c/\eta$

$\mathcal{E}_c$ set of energy levels for the EVs belonging to class c, $\mathcal{E}_c = L_c^{max}/(\delta \cdot v_f)$

The power network sets

$\mathcal{P}_N$ set of buses

$\mathcal{P}_L$ set of distribution lines

$\Gamma(j)$ Successor set of bus j

Parameters

a_j, b_j	Energy production cost coefficients at bus j
$\mu(t)$	Contract electricity price with the main grid in period t
p_j^{ramp}	Ramp limits of generators at bus j

Variables

$p_j^g(t)$	Active power generation at bus j during period t
$p_j^{dc}(t)$	Charging load at bus j during period t
$P_{ij}(t)$	Active/Reactive power flowing from buses i to j during period t

Acronym

EVs	Electric Vehicles
FCSs	Fast Charging Stations
ERN	Electrified Road Network
PDN	Power Distribution Network

1. Introduction

Electric vehicles (EVs) are increasingly deployed worldwide [1], due to their potential contribution in reducing green house gas emission, increased economic viability and convenience for the users. However, this brings new challenges to both the transportation and power systems. EV drivers need to consider the charging cost and time at different charging stations, when planning their trips. Traffic patterns are affected by the electricity price and the locations of fast charging stations (FCSs). On the one hand, the spatial and temporal charging demand resulting from the EVs charging patterns impacts the distribution of power flow, which challenges the operation of the existing power systems. On the other hand, this provides opportunities to efficiently operate power systems through vehicle-to-grid exchanges which could stabilize the power flow under the conditions of increased integration of renewable energy. In this setting, the power systems and the electrified road

networks (ERNs) interact with each other through the dynamics of electricity price and charging demand. Such interplay brings challenges to control and operate the two systems, but also brings opportunities to promote integration and communication between each other.

Investigating how to model, operate and control the coupled ERNs and power systems considering EV charging has gained attention in recent years [2, 3, 4]. Some of the main challenges addressed in the literature are how to properly model the physical features of the coupled transportation systems and power systems, as well as, modeling EVs and EVs supply equipment.

Some studies only consider the ERNs, ignoring the technical constraints coming from the power systems. Their objectives are mainly of optimizing allocation of FCSs [5, 6, 7], charging navigation [8] and routing [9, 10], as well as simulating coordinated and uncoordinated charging modes [11]. Some studies, instead, only consider detailed power systems modeling including EVs charging load, without considering realistic features of ERNs. Some of the topics considered can be summarized as: 1) Investigating the impacts of EVs on power systems in terms of safety [12], reliability [13], normal operation [14], among others. 2) Long term planning problems [15], e.g., optimizing the allocation of smart grid components and charging stations [16, 17]; reinforcing power systems capacity to enable the massive deployment of solar photovoltaics, electric heat pumps and EVs [18], among others. 3) Coordinating EVs charging [19], such as, minimizing the number of coordinated EVs to mitigate voltage unbalance [20]; coordinating EVs charging while maintaining the voltage deviation within acceptable power quality limits [21]; managing day-ahead electricity procurement and real-time EVs charging to minimize the total operating cost [22]. In the majority of cases, the spatial and temporal charging demand are required to be estimated statistically from existing data, which is however difficult to access.

Other studies consider the coupled power systems and ERNs, and investigate the interdependency between the two systems [23]. Several frameworks [24, 25, 26] have been proposed to model the interaction of traffic-power systems, wherein in most models the traffic and power flow interact with each other through electricity price, charging load and traffic toll. In this paper, we consider that the traffic flow within the ERNs and the power flow are interdependent through the charging demand at each FCS and the associated locational marginal price (LMP). Within this interaction process, from an ERN operator's perspective, the dynamic electricity price (i.e., LMP) and the capacity of FCSs are important parameters. The former is obtained from

power systems and the latter is a key physical feature of an ERN. Both can influence the route choice of EV drivers and non-EV drivers, since EVs drivers share the limited capacity of a FCS, and EVs and non-EVs drivers share the limited capacities of roads. Therefore, traffic flow patterns are affected by both factors and, further impact the distribution of charging demand. From a power system operator's perspective, the accurate data of the spatial and temporal charging demand from an ERN can help to manage the electricity production and balance the power flow of the systems. The spatial and temporal charging loads affect the power flow distribution subject to power system constraints, such as limitation of the grid and generator capacities, as well as ramp limits of generators. The power flow distribution, in return, influences the LMP, which would further affect traffic flow distribution. In this way, the ERN and power system interact with each other and both FCSs and EVs play critical roles in this interdependent traffic-power systems. The former is the interface connecting the ERN and power system, and the latter acts as the power prompting the interplay between traffic and power flow. Therefore, properly modeling the detailed physical features of EVs and FCSs is important to adequately study the interaction between the ERN and the power system. Here, we list some of the critical features that need to be modeled when investigating the interdependency of traffic-power systems and how they have been considered in the literature. A detailed comparison of these features in the literature is listed in Table 1.

Dynamics (feature of the coupled systems): A dynamic traffic-power system model is required due to: 1) the spatial and temporal nature of EVs; 2) the time-varying evolution of traffic flow; 3) the ramp limits of power generators. Most existing studies only considered a static model [27, 28, 29, 30, 31], whereas recently increasing attention has been paid to modeling dynamic [32, 33] or semi-dynamic [34] traffic-power systems.

Charging time (feature of EV): It is part of the travel time cost, when the time value is considered. Refs. [30, 31] assumed that all EVs, had (A1) the same exogenously given fixed charging time. This assumption is marked as (A1).

Charging demand (feature of EV): It influences the charging cost for EV drivers, and influences power production as well as power flow distribution. Refs. [28, 30, 31, 29] assumed all EVs had (A2) the same exogenously given fixed charging demand; Refs. [32, 34, 29] assumed the charging demand was (A3) only related to traffic flow through the FCSs without considering the real charging needs. It could cause the EVs to charge multiple times with-

out considering the remaining battery capacity leading to an overestimation of the charging demand.

Driving range/Battery capacity (feature of EV): It influences the number of times an EV has to recharge during a trip.

Initial state of charge (**SoC**) (feature of EV): It influences whether it is required to recharge an EV at the beginning of the time horizon. If it has, the initial SoC of an EV influences which FCSs this EV is able to reach without running out of battery. Ref. [28] assumed (A4) an EV was able to reach any FCS. This assumption may result in the assigned charging point to be beyond the remaining driving range of an EV.

Mix of gasoline vehicles (**GVs**) (feature of an ERN): EVs and GVs compete for the limited road capacity.

Capacity of FCSs (feature of an ERN): EVs compete for the limited charging capacities at FCSs.

Additionally, several decision-making environments considered for co-operations of traffic-power systems are summarized in Table 1. *Centralized* decision-making environments describe a situation where there is a single operator who controls both ERNs and power systems in a fully integrated manner. Their objectives usually lead to a social optimum. $Information-sharing$ decision-making environments describe a situation where ERNs and power systems operate independently, but they can share their operation plans at the beginning of each time step [32] or at the beginning of the time horizon [28, 30, 33]. Their own plans do not need to change according to the received information. They also can exchange their plans for any number of rounds. The sufficient information-sharing in Table 1 means that both the ERN operator and the power system operator share their information until converging (e.g., the changes of traffic flow pattern and charging price are smaller than a threshold [28]) or meeting the maximum iteration rounds. Refs. [28, 30, 32] showed that, under the sufficient information-sharing situation, the solution approximates to an equilibrium between ERNs and power systems. Furthermore, Ref. [33] has proved that the social optimum is a general equilibrium if LMP is used in power systems, where the power system operator is a nonprofit one whose objective is to balance the electricity supply and demand under technical security constraints. Since the power system operator is welfare-minded, it can steer a selfish ERN operator towards the social optimum. More discussions are detailed in Refs. [33]. As shown in Table 1, a systematic analysis for the interaction of traffic-power systems under different decision-making environments is missing.

Table 1: Summary of considered factors in relevant literatures

references	decision-making environments	dynamics	EV features				ERNs features	
			charging time	charging demand	driving range	initial SoC	GVs	capacity of FCSs
[35]	centralized	✓	×	(A3)	×	×	×	×
[32]	limited information-sharing	✓	×	(A3)	×	×	×	✓
[36]	centralized	✓	(A1)	(A2)	×	×	×	✓
[34]	centralized	✓	×	(A3)	×	×	×	×
[27]	centralized	×	✓	✓	✓	✓	×	×
[28]	sufficient information-sharing	×	✓	(A2)	×	(A4)	✓	✓
[29]	centralized	×	×	(A3)	✓	✓	×	✓
[30]	sufficient information-sharing	×	(A1)	(A2)	×	×	✓	✓
[31]	centralized	×	(A1)	(A2)	×	×	✓	✓

To fill the research gaps mentioned above, this paper proposes a dynamic traffic-power system model and investigates the coordination of traffic-power systems under centralized, decentralized and information-sharing decision-making environments.

The main contributions of the paper are summarized as follows:

1) We propose a novel dynamic traffic-power system model, which is able to capture the spatial-temporal traffic flow evolution and charging demand. Dynamic models can provide more accurate charging load information compared to static ones.

2) Within the proposed model, an electric link transmission model (eLTM) is proposed to solve the system optimal dynamic traffic assignment (SO-DTA) problem. The critical features of EVs and ERNs, summarized in Table 1, are thoroughly considered. Moreover, the proposed model also considers the different classes of EVs with different driving ranges, chargers with different charging powers in a FCS and the charging process of EVs. These extensions allow the model to be used in various applications and at different granularities.

3) This paper systematically investigates the operation of traffic-power systems under centralized, decentralized and information-sharing decision-making environments. The corresponding objective functions under different decision-making environments are formulated. An iterative algorithm is proposed to solve the centralized optimization problem. We compare the three environments in terms of the charging congestion level at FCSs, charging price, charging demand, integration of renewable energy, among others.

The remainder of the article is structured as follows. Section 2 develops the traffic-power system model. Section 3 describes decentralized, centralized

and information-sharing decision-making environments. Section 4 illustrates a numerical example to show the application of the proposed model and compares the solutions under different decision-making environments. Finally, Section 5 provides some concluding remarks and future research directions.

2. Coupled traffic-power system

2.1. Link transmission model based system optimal dynamic traffic assignment problem

A road network with multiple sources (origins) and sinks (destinations) is denoted as $G(\mathcal{N}, \mathcal{A})$, where $\mathcal{N}$ and $\mathcal{A}$ are the sets of nodes and links, respectively. All links (nodes) in the road network are classified into three types: source, sink and general links (nodes). Within the road network, each source (sink) node attaches only one source (sink) link, and each source (sink) link connects to only one source (sink) node. $\mathcal{N}_R$ (resp. $\mathcal{N}_S$) and $\mathcal{A}_R$ ($\mathcal{A}_S$) denote the set of source (sink) nodes and source (sink) links, respectively. All source (sink) links are dummy of length zero and infinite outflow, inflow and storage capacities. For SO-DTA problems, the outflow capacity of all sink links are assumed to be 0, which means that all vehicles are collected upon their arrival. The time horizon H is discretized into a finite set of periods $\mathcal{T} = \{t = 1, 2, \cdots, T\}$. T is calculated according to $T = H/\delta$, where δ is the period length. The period length should be equal to or smaller than the smallest link travel time so that vehicles take at least one time unit to traverse a link [37].

A triangular fundamental diagram is used in the link transmission model (LTM) [37, 38], which is an approximation and describes a macroscopic property of roads considering the number of lanes, weather conditions, speed limits, among others [37]. The diagram is defined by three parameters: a jam density (k_{jam}), a maximum flow (q_{max}) and a fixed-free flow speed (v_f). The backward shock-wave speed w can be obtained by $w = q_{max} \cdot v_f/(q_{max} - k_{jam} \cdot v_f)$. The LTM updates the traffic flow evolution by calculating the cumulative number of vehicles at the entry and exit of each link in each period.

The Newell's simplified theory is used in LTM to calculate sending $S_a(t)$ and receiving $R_a(t)$ capacities of link a:

$$S_a(t) = \min\{U_a(t - \nu_a) - V_a(t - 1), Of_a(t)\} \tag{1a}$$

$$R_a(t) = \min\{V_a(t-\beta_a) + L_a \cdot k_{jam} - U_a(t-1), If_a(t)\} \tag{1b}$$

where $U_a(t)$ ($V_a(t)$) denotes the cumulative number of vehicles that enter (leave) link a by the end of period t, respectively. $If_a(t)$ and $Of_a(t)$ are the inflow capacity at the entering point and outflow capacity at the leaving point of link a during period t. They can be obtained by $\delta \cdot q_{max}$ at the corresponding location and period. L_a is the length of link a. ν_a is the free-flow travel time on link a and β_a is the travel time required by the backward shock wave from the exit to the entry of link a. They can be obtained by $\nu_a = L_a/(\delta \cdot v_f)$ and $\beta_a = L_a/(\delta \cdot w)$, respectively.

The inflow and outflow of link a during interval t are constrained by its corresponding sending and receiving capacities, respectively:

$$U_a(t) - U_a(t-1) \leq R_a(t), \forall a \in \mathcal{A}, t \in \mathcal{T} \tag{2a}$$

$$V_a(t) - V_a(t-1) \leq S_a(t), \forall a \in \mathcal{A}, t \in \mathcal{T} \tag{2b}$$

In the LTM-based SO-DTA problem, the different classes of vehicles are not distinguished. Thus, we have:

$$U_a(t) = \sum_{s \in \mathcal{N}_S} UG_a^s(t), \forall a \in \mathcal{A}, t \in \mathcal{T} \tag{3a}$$

$$V_a(t) = \sum_{s \in \mathcal{N}_S} VG_a^s(t), \forall a \in \mathcal{A}, t \in \mathcal{T} \tag{3b}$$

where $UG_a^s(t)(VG_a^s(t))$ denotes the cumulative number of gasoline vehicles that enter(leave) link a to destination s by the end of period t.

Substituting Eqs. (1) and (3) into the inequalities in Eq. (2), the linear LTM-based flow constraints are obtained as follows:

$$\sum_{s \in \mathcal{N}_S} VG_a^s(t) \leq \sum_{s \in \mathcal{N}_S} UG_a^s(t-\nu_a), \forall a \in \mathcal{A}, t \in \mathcal{T} \tag{4}$$

$$\sum_{s \in \mathcal{N}_S} [VG_a^s(t) - VG_a^s(t-1)] \leq Of_a(t), \forall a \in \mathcal{A}, t \in \mathcal{T} \tag{5}$$

$$\sum_{s \in \mathcal{N}_S} UG_a^s(t) \leq \sum_{s \in \mathcal{N}_S} VG_a^s(t-\beta_a) + L_a \cdot k_{jam}, \forall a \in \mathcal{A}, t \in \mathcal{T} \tag{6}$$

$$\sum_{s\in\mathcal{N}_S}[UG_a^s(t)-UG_a^s(t-1)]\le If_a(t),\forall a\in\mathcal{A},t\in\mathcal{T} \tag{7}$$

The cumulative outflow to destination s should be constrained by the cumulative inflow to the same destination on link a:

$$VG_a^s(t)\le UG_a^s(t-\nu_a),\forall a\in\mathcal{A},t\in\mathcal{T} \tag{8}$$

The traffic demand is satisfied by letting the cumulative inflows of source links equal to the cumulative demands:

$$UG_a^s(t)=DG_a^s(t),\forall a\in\mathcal{A}_R,\forall s\in\mathcal{N}_S,t\in\mathcal{T} \tag{9}$$

where $DG_a^s(t)$ is the cumulative gasoline vehicle travel demand between the entry of origin link a and destination s at the end of period t.

In the LTM model, the inflow and outflow of a general node should be restricted by the following flow conservation constraints:

$$\sum_{a\in B(i)}VG_a^s(t)=\sum_{b\in A_(i)}UG_a^s(t),\forall i\in\mathcal{N}/\{\mathcal{N}_R,\mathcal{N}_S\},\forall s\in\mathcal{N}_S,t\in\mathcal{T} \tag{10}$$

where $A(i)$ ($B(i)$) represents the set of links whose tail (head) node is i.

The cumulative flows should be nonnegative and nondecreasing :

$$VG_a^s(t)-VG_a^s(t-1)\ge 0,\forall a\in\mathcal{A},\forall s\in\mathcal{N}_S,t\in\mathcal{T} \tag{11}$$

$$UG_a^s(t)-UG_a^s(t-1)\ge 0,\forall a\in\mathcal{A},\forall s\in\mathcal{N}_S,t\in\mathcal{T} \tag{12}$$

The following constraints force the initial cumulative flows to be 0:

$$UG_a^s(0)=VG_a^s(0)=0,\forall a\in\mathcal{A},\forall s\in\mathcal{N}_S \tag{13}$$

The objective of the LTM-based SO-DTA problem is to minimize the total travel time of all vehicles. The total travel time is calculated by the total presence time of all vehicles on all links during the whole time horizon. The LTM-based SO-DTA problem [38] is formulated as follows:

$$\min_{\boldsymbol{x}\in\Omega}\sum_{a\in\mathcal{A}/\mathcal{A}_S}\sum_{s\in\mathcal{N}_S}\sum_{t\in\mathcal{T}}\delta[UG_a^s(t)-VG_a^s(t)] \tag{14}$$

where $\Omega=\{\boldsymbol{x}|\text{ s.t. }(4)-(13)\}$.

2.2. eLTM-based SO-DTA problem

The existing LTM-based SO-DTA model is not able to describe the new features related to the EVs, such as the driving range of EVs and the capacity of FCSs. To overcome this shortcoming, an eLTM-based SO-DTA model is proposed to minimize the total cost for all vehicles considering the EVs driving ranges, FCS capacities, charging costs, among others.

The assumptions in this model are:

(1) An EV charges the minimum en-route to ensure the shortest travel time. The SoC after charging (original SoC plus the charged electricity) should ensure that the EV can reach the destination or the next FCS. This assumption is coherent with the objective function of the proposed model, which is to minimize the total cost. Other phenomena, e.g., the EVs only leave FCSs after being fully charged or 80% charged, can be easily incorporated by adding constraints on FCSs. As for the heterogeneous charging preferences of EV drivers, their consideration is not within the scope of this paper.

(2) The electricity consumed by an EV is linearly related to the distance traveled. The electricity amount charged by an EV is linearly related to the charging time. All EV batteries have the same energy consumption efficiency, similar to Ref. [39].

(3) The electricity consumed by the in-vehicle equipment, such as air conditioners and lights, is neglected. When EVs stop, no electricity is consumed.

In order to track the SoC of EVs, the model accounts for different energy levels to describe the real-time SoC for each EV. Given a certain class of EV denoted as c, its battery capacity is B_c kWh and the energy consumption efficiency is η kWh/mile: then, the mileage of this class EV is $B_c/\eta = L_c^{max}$ miles. One energy level (EL) is defined to be equal to $\delta \cdot v_f$ miles. Therefore, the maximum EL of EV of class c is calculated by $E_c = L_c^{max}/(\delta \cdot v_f)$. Assuming that there are C EV classes represented as $\mathcal{C} = \{\mathcal{E}_1, \mathcal{E}_2, \cdots, \mathcal{E}_C\}$, each element in set $\mathcal{C}$ is a set, which contains the energy levels that EV of class c could have, denoted as $\mathcal{E}_c = \{1, 2, \cdots, E_c\}$.

To describe the FCS in the physical road network, dummy charging links $\mathcal{A}_C$ are originally defined in the eLTM-based model. A FCS is modeled by one or several charging links, represented by arcs having the same origin and destination, as shown in Fig. 1. Chargers with different charging speeds are represented by different charging links. Parameter α_a^t represents the average charging speed for each charging link a during period t, which translates

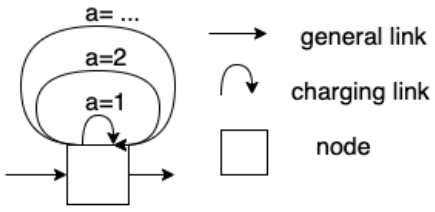

Figure 1: Link representation of different types of charges within a charging station.

to how many energy levels can be supplied using type a charger during a period δ. Assuming the charging power of charging link a is p_a^{ev}, then, α_a^t can be calculated by $\frac{p_a^{ev} \cdot \delta}{\eta \cdot \delta \cdot v_f} = \frac{p_a^{ev}}{\eta \cdot v_f}$. Similar to source and sink links, the lengths of charging links are assumed to be 0. For each charging link a, $NC_a(t)$ is defined as the physical number of type a chargers during period t. Generally, charging speed α_a^t and number of chargers $NC_a(t)$ are a constant and only change with charging links. However, if some chargers temporally or permanently are unavailable (e.g., due to physical failures, maintenance and upgrade), these parameters could change over time.

Given a general link a, its length is L_a and the energy consumption efficiency of EVs is η; then, the consumed ELs on link a is calculated by $\rho_a = L_a/\eta$. Similarly, $EU_{a,c}^{s,e}(t)$ ($EV_{a,c}^{s,e}(t)$) denotes the cumulative number of EVs that belong to type c with EL e that enter (leave) link a to destination s by the end of interval t.

In the eLTM-based model, both EVs and conventional vehicles are considered. Therefore, Eq. (3) is reformulated as follows :

$$U_a(t) = \sum_{s \in \mathcal{N}_S} UG_a^s(t) + \sum_{s \in \mathcal{N}_S} \sum_{c \in \mathcal{C}} \sum_{e \in \mathcal{E}_c} UE_{a,c}^{s,e}, \forall a \in \mathcal{A}, t \in \mathcal{T} \tag{15a}$$

$$V_a(t) = \sum_{s \in \mathcal{N}_S} VG_a^s(t) + \sum_{s \in \mathcal{N}_S} \sum_{c \in \mathcal{C}} \sum_{e \in \mathcal{E}_c} VE_{a,c}^{s,e}, \forall a \in \mathcal{A}, t \in \mathcal{T} \tag{15b}$$

Substituting Eqs. (1) and (15) into the inequalities in Eq. (2), the eLTM-based flow constraints for EVs and aggregate vehicle flows are obtained as

follows:

$$VE_{a,c}^{s,e}(t) \leq UE_{a,c}^{s,e+\rho_a}(t-\nu_a), \forall a \in \mathcal{A}\backslash\{\mathcal{A}_C\}, \\ \forall s \in \mathcal{N}_S, \forall c \in \mathcal{C}, e \in \mathcal{E}_c \cap \{e \leq E_c - \rho_a\}, t \in \mathcal{T} \tag{16a}$$

$$VE_{a,c}^{s,e}(t) = 0, \forall a \in \mathcal{A}\backslash\{\mathcal{A}_C\}, \\ \forall s \in \mathcal{N}_S, \forall c \in \mathcal{C}, e \in \mathcal{E}_c \cap \{e > E_c - \rho_a\}, t \in \mathcal{T} \tag{16b}$$

$$\sum_{s\in\mathcal{N}_S}[VG_a^s(t) - VG_a^s(t-1)] + \sum_{s\in\mathcal{N}_S}\sum_{c\in\mathcal{C}}\sum_{e\in\mathcal{E}_c}[VE_{a,c}^{s,e}(t) - VE_{a,c}^{s,e}(t-1)] \\ \leq Of_a(t), \forall a \in \mathcal{A}\backslash\{\mathcal{A}_C\}, t \in \mathcal{T} \tag{17}$$

$$\sum_{s\in\mathcal{N}_S}\sum_{c\in\mathcal{C}}\sum_{e\in\mathcal{E}_c}[UE_{a,c}^{s,e}(t) - VE_{a,c}^{s,e}(t-\beta_a)] + \\ \sum_{s\in\mathcal{N}_S}[UG_a^s(t) - VG_a^s(t-\beta_a)] \leq L_a k_{jam}, \forall a \in \mathcal{A}\backslash\{\mathcal{A}_C\}, t \in \mathcal{T} \tag{18}$$

$$\sum_{s\in\mathcal{N}_S}[UG_a^s(t) - UG_a^s(t-1)] + \\ \sum_{s\in\mathcal{N}_S}\sum_{c\in\mathcal{C}}\sum_{e\in\mathcal{E}_c}[UE_a^s(t) - UE_a^s(t-1)] \leq If_a(t), \forall a \in \mathcal{A}\backslash\{\mathcal{A}_C\}, t \in \mathcal{T} \tag{19}$$

Eq. (16a) guarantees that the outflow should be less than or equal to the inflow and that the consumed ELs are deducted after EVs traversed the corresponding links. Eq. (16b) ensures that EV ELs are less than their maximum ELs. Eqs. (17) - (19) are same as Eqs. (5) - (7). Eqs. (17) and (19) constrain the outflow and inflow to be less than or equal to their outflow and inflow capacities, respectively. Eq. (18) states that the number of vehicles on link a should be less than or equal to the maximum number of vehicles that can be contained on this link.

Eq. (20) ensures that traffic demand of EVs should also be satisfied:

$$UE_{a,c}^{s,e}(t) = DE_{a,c}^{s,e}(t), \forall a \in \mathcal{A}_R, \forall s \in \mathcal{N}_S, \forall c \in \mathcal{C}, \forall e \in \mathcal{E}_c, t \in \mathcal{T} \tag{20}$$

Similar to Eq. (10), the flow conservation law should also be followed by

EVs:

$$\sum_{a\in B(i)} VE_{a,c}^{s,e}(t) = \sum_{b\in A_{(i)}} UE_{a,c}^{s,e}(t), \\ \forall i \in \mathcal{N}/\{\mathcal{N}_R, \mathcal{N}_S\}, \forall s \in \mathcal{N}_S, \forall c \in \mathcal{C}, \forall e \in \mathcal{E}_c, t \in \mathcal{T} \tag{21}$$

2.2.1. Modeling EV charging process

To model the charging process, intermediate variables $\hat{x}_{a,s}^{s,e}(t)$ and $x_{a,s}^{s,e}(t)$ are defined as the number of EVs before and after their ELs have been updated on charging link a. The occupancy $\hat{x}_{a,s}^{s,e}(t)$ on a charging link is calculated by the occupancy plus new inflow minus outflow during the previous period, as shown in Eq. (22):

$$\hat{x}_{a,s}^{s,e}(t) = x_{a,s}^{s,e}(t-1) + [UE_{a,c}^{s,e}(t-1) - UE_{a,c}^{s,e}(t-2)] - \\ [VE_{a,c}^{s,e}(t-1) - VE_{a,c}^{s,e}(t-2)], \\ \forall a \in \mathcal{A}_C, \forall s \in \mathcal{N}_S, \forall c \in \mathcal{C}, \forall e \in \mathcal{E}_c, t \in \mathcal{T} \tag{22}$$

Furthermore, the following equations describe the process of updating the ELs on charging links:

$$x_{a,c}^{s,E_c}(t) = \sum_{l=0}^{\alpha_a^t} \hat{x}_{a,c}^{s,E_c-l}(t), \ \forall a \in \mathcal{A}_C, \forall s \in \mathcal{N}_S, \forall c \in \mathcal{C}, \forall t \in \mathcal{T} \tag{23a}$$

$$x_{a,c}^{s,e}(t) = \hat{x}_{a,c}^{s,e-\alpha_a^t}(t), \ \forall a \in \mathcal{A}_C, \forall s \in \mathcal{N}_S, \forall c \in \mathcal{C}, \forall e \in \{\alpha_a^t \le e < E_c\}, \forall t \in \mathcal{T} \tag{23b}$$

$$x_{a,c}^{s,e}(t) = 0, \forall a \in \mathcal{A}_C, \forall s \in \mathcal{N}_S, \forall c \in \mathcal{C}, \forall e \in \{e < \alpha_a^t\}, \forall t \in \mathcal{T} \tag{23c}$$

Eqs. (23a) and (23c) constrain the upper and lower bounds of the updated ELs. Eqs. (23b) describe the process of linear increase in ELs. Eq. (23a) states that if the ELs of EVs before being updated belong to $[E_c - \alpha_a^t, E_c]$, their energy levels are approximately updated as the maximum EL E_c of EV of class c after one period. Eq. (23b) states that if the ELs of EVs are within $[0, E_c - \alpha_a^t)$ before being updated, they increase α_a^t ELs after one period. The updated ELs are within $[\alpha_a^t \le e < E_c)$. Eq. (23c) ensures that no EVs' ELs are less than α_a^t level after being charged for one period. Therefore, if the updated ELs are smaller than α_a^t, they are forced to be 0. Note that the number of EVs on charging links are conserved before and after the ELs of

the EVs are updated, i.e., $\sum_e \hat{x}^{s,e}_{a,c}(t) = \sum_e x^{s,e}_{a,c}(t)$.

Additionally, the outflow disaggregated by each EL on charging link a should be less than its occupancy, as formulated in Eq. (24):

$$VE^{s,e}_{a,c}(t) - VE^{s,e}_{a,c}(t-1) \leq x^{s,e}_{a,c}(t), \forall a \in \mathcal{A}_C, \forall s \in \mathcal{N}_S, \forall c \in \mathcal{C}, \forall e \in \mathcal{E}_c, \forall t \in \mathcal{T} \tag{24}$$

Eq. (25) limits the number of EVs on charging link a to its maximum number of chargers:

$$\sum_{s \in \mathcal{N}_S} \sum_{c \in \mathcal{C}} \sum_{e \in \mathcal{E}_c} [UE^{s,e}_{a,c}(t) - VE^{s,e}_{a,c}(t)] \leq NC_a(t), \forall a \in \mathcal{A}_C, \forall t \in \mathcal{T} \tag{25}$$

Moreover, Eqs. (26) - (27) ensure that the cumulative EV flows are nonnegative and nondecreasing:

$$VE^{s,e}_{a,c}(t) - VE^{s,e}_{a,c}(t-1) \geq 0, \forall a \in \mathcal{A}, \forall s \in \mathcal{N}_S, \forall c \in \mathcal{C}, \forall e \in \mathcal{E}_c, t \in \mathcal{T} \tag{26}$$

$$UE^{s,e}_{a,c}(t) - UE^{s,e}_{a,c}(t-1) \geq 0, \forall a \in \mathcal{A}, \forall s \in \mathcal{N}_S, \forall c \in \mathcal{C}, \forall e \in \mathcal{E}_c, t \in \mathcal{T} \tag{27}$$

Similarly, the occupancies on charging links is nonnegative, as described in Eq. (28):

$$x^{s,e}_{a,c}(t) \geq 0,\ \hat{x}^{s,e}_{a,c}(t) \geq 0, \forall a \in \mathcal{A}_C, \forall s \in \mathcal{N}_S, \forall c \in \mathcal{C}, \forall e \in \mathcal{E}_c, t \in \mathcal{T} \tag{28}$$

The occupancies on charging links and the cumulative EV flows are initialized to be 0, as formulated in Eq. (29):

$$UE^{s,e}_{a,c}(0) = VE^{s,e}_{a,c}(0) = 0, \forall a \in \mathcal{A}, \forall s \in \mathcal{N}_S, \forall c \in \mathcal{C}, \forall e \in \mathcal{E}_c \tag{29}$$

As for the LTM-based SO-DTA problem, the objective of the eLTM-based SO-DTA problem is to minimize the total travel time, including the charging time of EVs. The problem is formulated as:

$$\begin{aligned} \min_{\boldsymbol{y} \in \Psi} & \sum_{s \in \mathcal{N}_S} \sum_{t \in \mathcal{T}} \sum_{a \in \mathcal{A}/\{\mathcal{A}_C, \mathcal{A}_S\}} \delta[UG^s_a(t) - VG^s_a(t)] \\ + & \sum_{s \in \mathcal{N}_S} \sum_{t \in \mathcal{T}} \sum_{a \in \mathcal{A}/\mathcal{A}_S} \sum_{c \in \mathcal{C}} \sum_{e \in \mathcal{E}_c} \delta[UE^{s,e}_{a,c}(t) - VE^{s,e}_{a,c}(t)] \end{aligned} \tag{30}$$

where $\Psi = \{\boldsymbol{y}|$ s.t. (8) − (13) and (16) − (29)$\}$. It should be noted that for all a in constraints (8)-(13) its domain does not include $\mathcal{A}_C$. It means conventional vehicles never go into charging links.

2.3. Power distribution network (PDN) model

We consider a radial PDN $\mathcal{G}_P(\mathcal{P}_N, \mathcal{P}_L)$, where $\mathcal{P}_N$ and $\mathcal{P}_L$ represent the sets of buses and distribution branches, respectively. In a radial network, each bus is attached to a unique predecessor bus and the number of buses equals to that of branches, which excludes a slack bus. Slack bus is indexed as 0. The successor set of bus j is denoted as $\Gamma(j) = \{\forall k : (j,k) \in \mathcal{P}_L\}$. The power system model in Ref. [28] is employed in this paper. We additionally add constraint (31) to limit the generator ramp between two successive periods:

$$-p_j^{ramp} \leq p_j^g(t) - p_j^g(t-1) \leq p_j^{ramp}, \forall j \in \mathcal{P}_N, \forall t \in \mathcal{T} \tag{31}$$

where p_j^g is the active power generation in period t and p_j^{ramp} is the ramp limits of generators at bus j.

The EV charging load in Ref. [28] is calculated by the static traffic flow passing charging stations and the energy demand of each EV is assumed to be fixed. In our paper, the charging load during each period is calculated by the number of EVs stoping in charging links. The energy demand of each EV is consistent with assumption (1) in subsection 2.2. Thus, the EV charging load in Eq. (28) in Ref. [28] is replaced by the following equation:

$$p_j^{dc}(t) = \sum_{a \in M(j)} \sum_{s \in \mathcal{N}_S} \sum_{c \in \mathcal{C}} \sum_{e \in \mathcal{E}_c} p_a^{ev} [UE_{a,c}^{s,e}(t) - VE_{a,c}^{s,e}(t)] \tag{32}$$

where $M(j)$ is a mapping from bus set $\mathcal{P}_N$ to charging links set $\mathcal{A}_C$, which specifies the connection between buses in a power system and charging links in a road network. $N(a)$ is a reverse mapping of $M(j)$, which maps charging links set to the bus set. The LMP at each bus is denoted as λ_j^t. The charging price at charging link a can be obtained by $\lambda_{N(a)}^t$.

To clearly describe the PDN model here, we detail the objective function used. The objective of the PDN operator is to minimize the total energy production costs. The optimal power flow problem is defined as **P1**:

$$\min_{\boldsymbol{z} \in \Phi} \sum_{t \in \mathcal{T}} \sum_{j \in \mathcal{P}_N} [a_j (p_j^g(t))^2 + b_j p_j^g(t)] + \sum_{t \in \mathcal{T}} \sum_{k \in \Gamma(0)} \mu(t) P_{0k}(t) \tag{33}$$

$$\Phi = \{\boldsymbol{z}| \text{ s.t. } (31)-(32), \text{ and } (24)-(34) \text{ in Ref. [24]}\} \tag{34}$$

where a_j and b_j are the production cost coefficients at bus j. P_{0k} is the active power flow from main grid to bus k. The first term is the production cost of the local generators and the second term is the cost for purchasing electricity from the main grid. $\mu(t)$ is the contract energy price during period t with the main grid.

3. Decision environments

In this section, three decision-making environments are considered for operating the traffic-power systems, which may arise when different beneficiaries coordinate the interdependent infrastructures. Analyzing different decision-making environments allows us to compare their operational and socially beneficial difference. The value of sharing information also can be studied.

3.1. Decentralized decision environments

In current practice, individual infrastructure systems such as ERNs and PDNs often determine their operation in an independent, decentralized manner with little information exchange among them.

For the ERN sector, we adopt a system optimum model where the objective is to minimize the total travel cost through dynamic traffic assignment. The total travel cost includes the driving time cost of both EVs and GVs, charging time cost of EVs and charging cost of EVs. This optimal traffic flow problem **P2** is formulated as follows:

$$\begin{aligned}
&\min_{\boldsymbol{y}\in\Psi} \sum_{s\in\mathcal{N}_S}\sum_{t\in\mathcal{T}}\sum_{a\in\mathcal{A}/\{\mathcal{A}_C,\mathcal{A}_S\}} \phi\delta[UG_a^s(t) - VG_a^s(t)] \\
&+\sum_{s\in\mathcal{N}_S}\sum_{t\in\mathcal{T}}\sum_{a\in\mathcal{A}/\mathcal{A}_S}\sum_{c\in\mathcal{C}}\sum_{e\in\mathcal{E}_c} \phi\delta[UE_{a,c}^{s,e}(t) - VE_{a,c}^{s,e}(t)]+ \\
&\sum_{s\in\mathcal{N}_S}\sum_{t\in\mathcal{T}}\sum_{c\in\mathcal{C}}\sum_{e\in\mathcal{E}_c}\sum_{a\in\mathcal{A}_C} \lambda_{N(a)}^t p_a^{ev}\delta[UE_{a,c}^{s,e}(t) - VE_{a,c}^{s,e}(t)]\}
\end{aligned} \tag{35}$$

subject to constraints (8)-(13) and (16)-(29), where ϕ is the time value.

Since the ERN operator does not know the real-time electricity price $\lambda_{N(a)}^t$ beforehand, we assume that an estimated fixed charging price is used for the

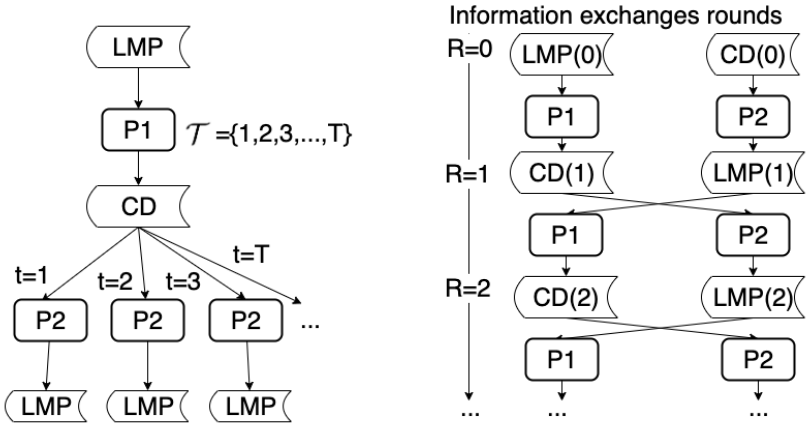

(a) Procedures of decentralized decision-making environment

(b) Procedures of information-sharing decision-making environment

Figure 2: Procedures of decentralized and information-sharing decision-making environments. CD: Charging demand of EVs; LMP: locational marginal price.

operator. For the PDN, it is assumed that the operator only knows the real-time charging demand and the demand in the future time periods is unknown. Thus, **P1** is solved for each independent period for a total of T times. The main process is shown in Fig. 2(a). At the beginning, the estimated charging price (LMP) for the ERN operator is used to solve **P1**. Then, in each period, the PDN operator receives the real-time charging demand from each FCS. Based on the real-time power demand, the operator solves **P2** to obtain the optimal power flow pattern $\boldsymbol{z}$ and the corresponding actual LMP in each period. Note that this price dose not change the traffic assignment solutions. In the end, the actual charging cost for the ERN operator can be calculated by the actual LMP.

3.2. Centralized decision environments

The centralized decision-making environment assumes that there is a centralized operator that coordinates both the ERNs and the PDNs to minimize the total cost of the two systems. It means that ERNs and PDNs fully integrate with each other, although this may lead to sacrifice their own benefits from an independent system's perspective. This situation may be ideal, but the results can serve as a benchmark to understand and analyze the best

possible coordination between ERNs and PDNs. This environment can be expressed as the following optimization problem:

$$\begin{aligned}
&\min_{\boldsymbol{y},\boldsymbol{z}\in\Psi,\Phi} \sum_{s\in\mathcal{N}_S}\sum_{t\in\mathcal{T}}\sum_{a\in\mathcal{A}/\{\mathcal{A}_C,\mathcal{A}_S\}} \phi\delta[UG_a^s(t)-VG_a^s(t)] \\
&+\sum_{s\in\mathcal{N}_S}\sum_{t\in\mathcal{T}}\sum_{a\in\mathcal{A}/\mathcal{A}_S}\sum_{c\in\mathcal{C}}\sum_{e\in\mathcal{E}_c}\phi\delta[UE_{a,c}^{s,e}(t)-VE_{a,c}^{s,e}(t)]+ \\
&\sum_{s\in\mathcal{N}_S}\sum_{t\in\mathcal{T}}\sum_{c\in\mathcal{C}}\sum_{e\in\mathcal{E}_c}\sum_{a\in\mathcal{A}_C}\lambda_{N(a)}^t p_a^{ev}\delta[UE_{a,c}^{s,e}(t)-VE_{a,c}^{s,e}(t)]\} \\
&+\sum_{t\in\mathcal{T}}\sum_{j\in\mathcal{P}_N}[a_j(p_j^g(t))^2+b_jp_j^g(t)]+\sum_{t\in\mathcal{T}}\sum_{k\in\Gamma(0)}\mu(t)P_{0k}(t)
\end{aligned} \tag{36}$$

subject to constraints (8)-(13), (16)-(29) and (34).

Since variables $\lambda_{N(a)}^t$ can be only obtained after the optimal power flow $\boldsymbol{z}$ has been known, an iterative algorithm is proposed to solve this problem. The main procedures of the algorithm is listed in Algorithm 1.

Algorithm 1: An iterative algorithm

1 Initialization:Chose a convergence tolerance $\epsilon > 0$ and the maximum iteration number I_{max}. Let LMP vector $\boldsymbol{\lambda} = 0$, objective value $\theta = 0, i = 0$;
2 Solve problem (36) with fixed LMP $\boldsymbol{\lambda}$; Get the objective value θ^* and retrieve $\boldsymbol{\lambda}^*$ from optimal power flow ;
3 **if** $|\theta - \theta^*| < \epsilon$ *for* N *consecutive times* **then**
4 | terminate and return the solution of problem (36);
5 **else if** $i = I_{max}$ **then**
6 | terminate, report that the algorithm fails to converge and return the solution of problem (36);
7 **else** $i = i + 1, \theta = \theta^*, \boldsymbol{\lambda} = \boldsymbol{\lambda}^*$, go to Line 2;

3.3. Information-sharing decision environments

The information-sharing decision-making environment describes a situation where an ERN operator and a PDN operator actively share (partial information about) their operation plans with each other, but do not necessarily fully coordinate or cooperate with each other. This environment

assumes that the two operators exchange their expected plans at the beginning of the time horizon. Specifically, an ERN operator sends the expected charging demands information to the PDN operator. Based on the received information, the PDN operator calculates the expected electricity prices and communicate them to the ERN operator who updates its plan accordingly. This information-sharing behavior can be continued for any number of rounds and the number of rounds can be understood as time available for the operators to exchange information. From a modeling perspective, the information-sharing decision-making environment is similar to the decentralized decision-making environment. Under both environments, the charging demand and LMPs are parameters for $\boldsymbol{P1}$ and $\boldsymbol{P2}$, respectively. The difference is that in the former environment, the PDN operator is able to know the possible charging demand over the whole time horizon at the beginning; whereas, in the latter environment, the PDN operator only knows the real-time charging demand during each period. The interplay process is shown in Fig. 2(b).

4. Numerical examples and results

4.1. Case study and system configuration

The similar structures of the ERN (with modified road lengths) and the radial PDN (with added renewable generators) in Ref. [28] is used to illustrate the proposed methods. The data used in the examples is briefly summarized in Appendix A. More detailed data and parameters are available in Supplementary Material [40]. We consider 4 renewable distributed generators (DGs) and 4 conventional generators connected to 4 renewable FCS (charging link label: 65, 67, 70, 72) and 4 conventional FCS (66, 68, 69, 71), respectively. In this example, we consider similar assumptions to Ref. [27]: 1) the DGs' outputs are assumed to be controllable which means the renewable power can be curtailed; 2) the available generation capacities of DGs are assumed to be given by proper forecasting methods, which provide the upper limits of the actual generation. The generation costs of both conventional and renewable DGs are detailed in Ref. [27].

4.2. Implementation note and results

All of the experiments have been run on a computer with an Intel Core i7-8700 3.2-GHz CPU with 32 GB of RAM. All of the problems have been solved by the commercial software IBM ILOG CPLEX (version 12.6).

Table 2: Summary of the main results under different decision-making environments

Decision environments	Cost ($)				Generation and purchase (MWh)		
	Actual charging cost	Actual traffic cost	Power cost	Actual total cost	Electricity purchase	Conventional DG	Renewable DG (%)
Decentralized	2556.78	11770.78	3924.15	15694.93	0.46	25.71	227.99(89.70%)
Centralized	183.74	9821.34	3065.80	12887.15	0.078	20.35	232.96(91.94%)
Information-sharing	245.21	9463.21	3924.15	13387.36	0.46	25.71	228.01(89.71%)

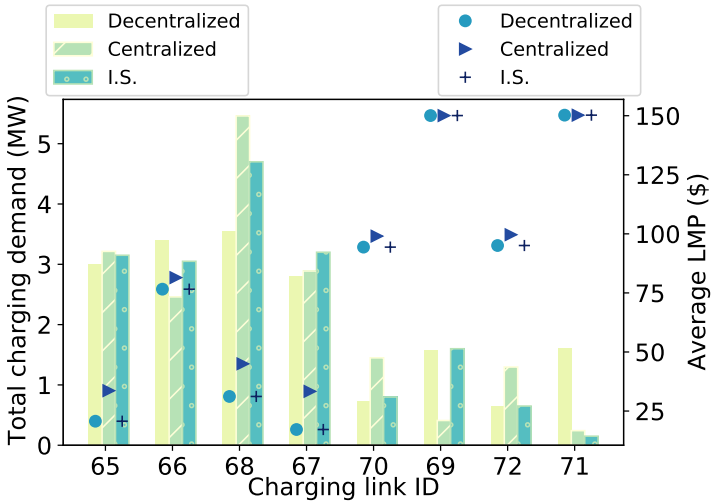

Figure 3: Total charging demand and average LMP in FCSs.

Algorithm 1 is employed to compute problem (36). The convergence tolerance ϵ and the maximum iteration number I_{max} are set as 0.01 and 90, respectively. Theoretically, information could be exchanged for any number of rounds between system operators; however, it is reasonable to assume that they only exchange information once due to practical limitations, particularly with respect to time.

Table 2 compares the results under the three decision-making environments. As it shows, we have the highest actual total cost $15694.93 when ERNs and PDNs operate independently. The total cost is 27.73% and 17.24% higher under the independent situation, compared to full integration or sharing information, respectively. This is because under the decentralized decision-making environment, the ERN operator only knows the fixed electricity price and has no information on the difference among FCSs and

Table 3: Total charging demand in renewable and conventional FCSs (MWh)

Environments	Renewable FCS (%)	Conventional FCS	Total
Decentralized	7.175 (41.47%)	10.125	17.3
Centralized	8.85(50.80%)	8.57	17.42
Information-sharing	7.8(45.09%)	9.5	17.3

periods, which results in only travel time minimization being considered. This leads to the highest charging cost and power expenditure. When an ERN operator exchanges information once with a PDN operator before traffic assignment, a significant reduction in the actual charging cost of up to 90.41% can be achieved. This is because one round information-sharing between the two operators can provide valuable information on the electricity price difference among FCSs and periods, although the information may not be exactly right. Such information can guide the ERN operator to minimize the travel time cost and charging cost. Under a fully integrated-centralized environment, the actual charging cost and power cost could decrease of up to 92.81% and 21.87%, respectively. Moreover, Fig. 3 shows that the FCSs with lower charging prices are generally assigned with more charging demand, and this correlation is clearer under centralized situation than the information-sharing situation. However, some exceptions can be observed, for instance, while the electricity price in FCS #68 is not the cheapest, it still maintains most charging demand. This is because there is a trade-off between the saved charging cost and the extra time caused by detouring to the FCS with cheaper charging price. Only when the charging price is cheap enough, EVs would detour to this particular FCS.

In addition, Table 2 shows that the centralized decision-making environment has the highest renewable energy adoption. This can be explained by two reasons: first, a part of charging demand is shifted from conventional FCSs to renewable FCSs as shown in Table 3. The charging demand in renewable FCSs increase from 41.47% to 45.09% if the decision environment change from the decentralized to the centralized. More specifically, except FCS #68, the charging demands in the other three conventional FCSs (#66, #69 and #71) are shifted to renewable FCSs (#65, #67, #70 and #72) in varying degrees when the decision-making environments are centralized and information-sharing is on, as shown in Fig. 3. The second reason is that under the centralized decision-making environment, the system operator could

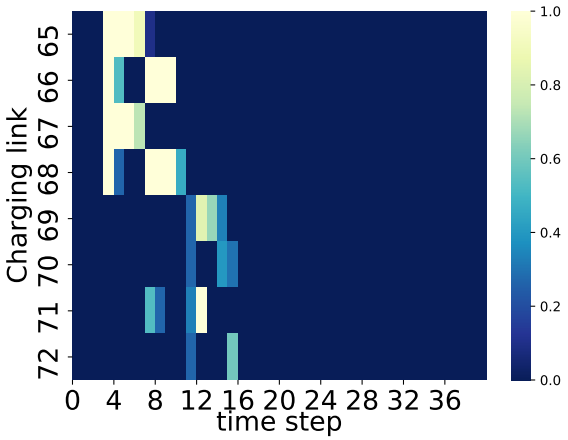

(a) Decentralized

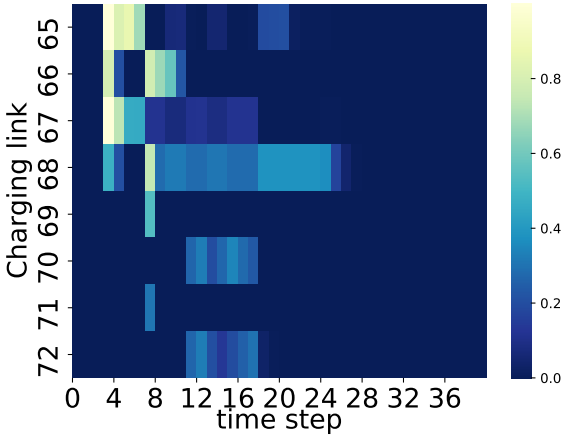

(b) Centralized

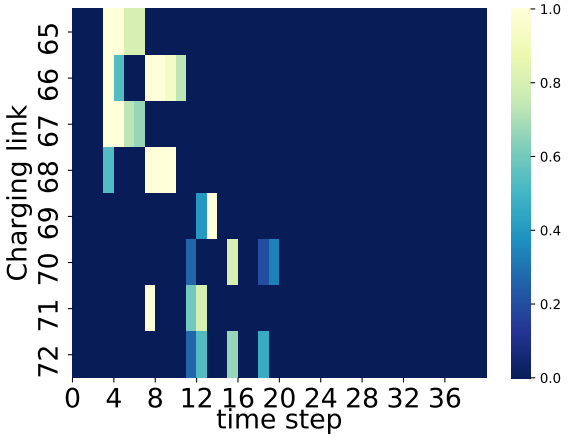

(c) Information-sharing

Figure 4: Congestion level of FCS under different decision-making environments.

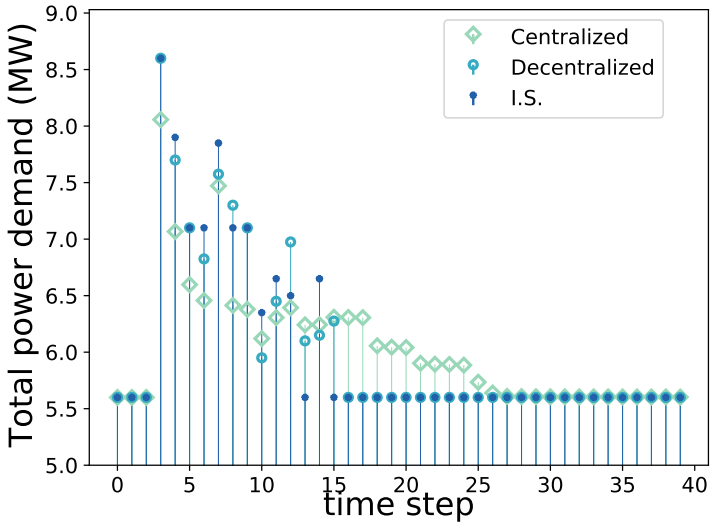

Figure 5: The time distribution of the total power demand for the studied PDN.

properly assign the charging time and locations of EVs so as to alleviate the charging congestion in FCSs in peak hours and flatten the the power demand curve. Note that the generation capacities of renewable DGs are limited in each period. Consequently, in peak hours, the expensive conventional energy could be replaced by the cheap renewable energy. This can be verified by Figs. 4 and 5. For example, the congestions in charging links 65, 67 and 68 are significantly alleviated when two systems operate jointly, as shown in Fig. 4. As a result, the total power demand from the 3rd to the 9th time step is clipped to from the 13rd to 26th time step, as shown in Fig. 5. In summary, the operator optimizes the charging demand in temporal and spatial aspects to promote the renewable energy integration and, thus, the total cost is minimized.

5. Conclusion

This paper proposed a traffic-power system model to investigate the operational solution differences when the electric road network (ERN) and the power distribution network (PDN) operate independently, jointly and with sharing information. The model considered constraints from both ERNs and PDNs, such as road capacity, traffic flow capacity and ramp limit of generators. Within this model, an electric link transmission model (eLTM) was

presented to solve the system optimal dynamic traffic assignment problem. A novel formulation was proposed to accommodate critical physical features of electric vehicles (EVs) and fast charging stations (FCSs), such as, EV classes with different driving ranges, initial state of charge (SoC) of EVs, capacity of FCSs have been considered. Moreover, the charging process of EVs was explicitly modeled within the eLTM. The objective of a PDN operator was to minimize the power cost including power generation cost and purchase from the main grid. A numerical example including renewable and conventional generators was studied to illustrate the proposed models. The different decision-making environments were compared to investigate the corresponding operation and social benefits. From the results, we could observe that the charging cost was the highest under decentralized situation, since the ERN operator did not know the information on the electricity price difference among FCSs and periods. Even limitedly sharing information or operating jointly between ERNs and PDNs could significantly reduce the charging cost. The increased renewable energy adoption and the flattened power demand curve assisted in lowering charging cost, power cost and congestion level in FCSs, under a centralized situation. Both electricity price difference among FCSs and detouring time influenced the charging demand distribution.

This work can be extended in several directions: 1) It is interesting to investigate by the proposed eLTM to solve the user equilibrium dynamic traffic assignment (UE-DTA) problem considering critical features of ERNs and FCSs. Although, Refs. [32, 36, 34] claimed that they have solved UE-DTA considering EVs, they oversimplified the critical features of ERNs and FCSs, as shown in Table 1. Therefore, how to solve this problem is still challenging. 2) The proposed models can be easily extended to investigate how the failure spreads between the interdependent traffic-power systems. 3) It is also interesting to investigate how to coordinate the charging demand so as to maximize the renewable energy adoption considering the security constraints and the weather conditions.

Appendix A. Data description

A modified electrified road network [28] and power distribution network is used to illustrated the proposed methods. Figs. A.6 and A.7 show the modified road network and power network. As shown in Fig. A.6, there is one type charger in each FCS. The green mark on charging links and generators represents the corresponding FCSs and generators powered by the renewable

Table A.4: Connections between charging links and Buses

Charging link	Bus
65	1
66	2
67	4
68	3
69	6
70	5
71	8
72	7

Table A.5: Parameters of the studied traffic-power system

Parameters	Values
v_f (m/h)	50
k_{jam}(veh/m)	214
δ (min)	6
q_{max} (veh/h/lane)	2160
p_a^{ev} (kW)	50
η (kMh/mile)	0.25
ϕ ($/h)	10
C	1
E_c	20
B_c (kWh)	25
$NC_a(t)$	15
α_a^t (ELs/δ)	4

energy. The detail connections between charging links and buses are listed in Table A.4. The parameters used in this paper are listed in Tables A.5 and A.6. For simplicity, we assume there is one type EV and its battery capacity is 25 KWh and maximum energy level is 20. Total traffic demand is listed in Table A.7. More detailed data of the studied road network and power network are available in Supplementary Material [40].

References

[1] International Energy Agency (IEA), Global ev outlook 2020, Tech. rep., IEA (June 2020).

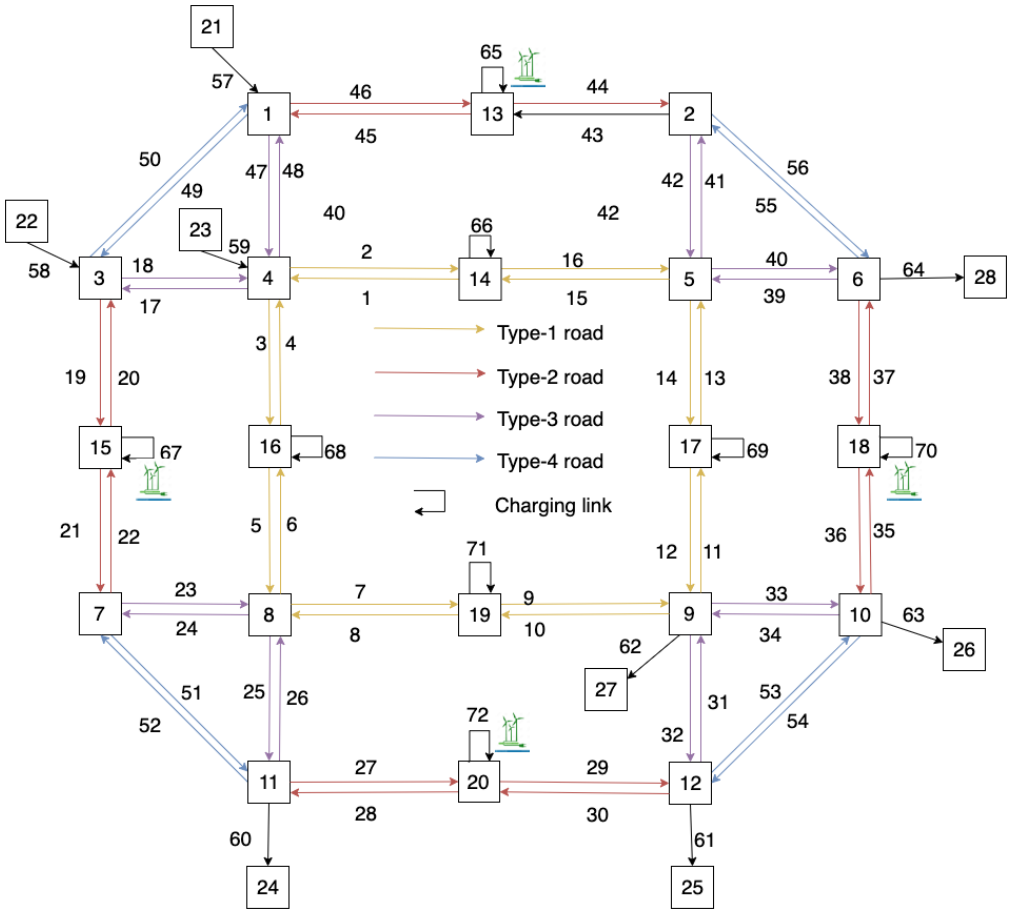

Figure A.6: The studied electrified road network.

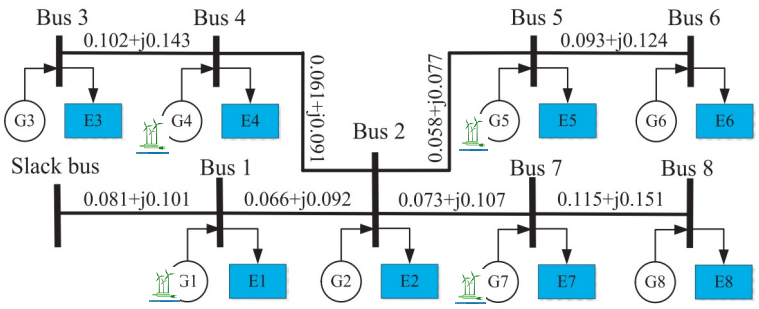

Figure A.7: The studied Power distribution network.

Table A.6: Parameters of the studied electrified road network

Road	Type-1	Type-2	Type-3	Type-4	Charging
ν_a	2	2	4	6	0
β_a	2	2	4	6	0
ρ_a	2	2	4	6	0

Table A.7: O-D pairs and their trip rates (in P.U.)

O-D pair	Conventional vehicles	EV	O-D pair	Conventional vehicles	EV
21-28	30	15	22-28	30	15
21-26	60	30	22-26	50	25
21-24	40	20	22-24	40	20
21-25	40	20	22-25	50	25
23-27	50	15	23-26	40	20
23-25	40	20			

[2] Y. Zheng, S. Niu, Y. Shang, Z. Shao, L. Jian, Integrating plug-in electric vehicles into power grids: A comprehensive review on power interaction mode, scheduling methodology and mathematical foundation, Renewable and Sustainable Energy Reviews 112 (2019) 424–439.

[3] F. Teng, Z. Ding, Z. Hu, P. Sarikprueck, Technical review on advanced approaches for electric vehicle charging demand management, part i: Applications in electric power market and renewable energy integration, IEEE Transactions on Industry Applications 56 (5) (2020) 5684–5694.

[4] Z. Ding, F. Teng, P. Sarikprueck, Z. Hu, Technical review on advanced approaches for electric vehicle charging demand management, part ii: Applications in transportation system coordination and infrastructure planning, IEEE Transactions on Industry Applications 56 (5) (2020) 5695–5703.

[5] R. Xie, W. Wei, M. E. Khodayar, J. Wang, S. Mei, Planning fully renewable powered charging stations on highways: A data-driven robust optimization approach, IEEE transactions on transportation electrification 4 (3) (2018) 817–830.

[6] R. Chen, X. Qian, L. Miao, S. V. Ukkusuri, Optimal charging facil-

ity location and capacity for electric vehicles considering route choice and charging time equilibrium, Computers & Operations Research 113 (2020) 104776.

[7] R. Vosooghi, J. Puchinger, J. Bischoff, M. Jankovic, A. Vouillon, Shared autonomous electric vehicle service performance: Assessing the impact of charging infrastructure, Transportation Research Part D: Transport and Environment 81 (2020) 102283.

[8] T. Qian, C. Shao, X. Wang, M. Shahidehpour, Deep reinforcement learning for ev charging navigation by coordinating smart grid and intelligent transportation system, IEEE Transactions on Smart Grid 11 (2) (2019) 1714–1723.

[9] M. M. Nejad, L. Mashayekhy, D. Grosu, R. B. Chinnam, Optimal routing for plug-in hybrid electric vehicles, Transportation Science 51 (4) (2017) 1304–1325.

[10] G. Hiermann, R. F. Hartl, J. Puchinger, T. Vidal, Routing a mix of conventional, plug-in hybrid, and electric vehicles, European Journal of Operational Research 272 (1) (2019) 235–248.

[11] L. Bedogni, L. Bononi, M. Di Felice, A. D'Elia, R. Mock, F. Morandi, S. Rondelli, T. S. Cinotti, F. Vergari, An integrated simulation framework to model electric vehicle operations and services, IEEE Transactions on vehicular Technology 65 (8) (2016) 5900–5917.

[12] B. Wang, P. Dehghanian, S. Wang, M. Mitolo, Electrical safety considerations in large-scale electric vehicle charging stations, IEEE Transactions on Industry Applications 55 (6) (2019) 6603–6612.

[13] A.-M. Hariri, M. A. Hejazi, H. Hashemi-Dezaki, Investigation of impacts of plug-in hybrid electric vehicles' stochastic characteristics modeling on smart grid reliability under different charging scenarios, Journal of Cleaner Production 287 (2021) 125500.

[14] D. Tang, P. Wang, Nodal impact assessment and alleviation of moving electric vehicle loads: From traffic flow to power flow, IEEE Transactions on Power Systems 31 (6) (2016) 4231–4242.

[15] V. H. Fan, Z. Dong, K. Meng, Integrated distribution expansion planning considering stochastic renewable energy resources and electric vehicles, Applied Energy 278 (2020) 115720.

[16] L. Luo, W. Gu, S. Zhou, H. Huang, S. Gao, J. Han, Z. Wu, X. Dou, Optimal planning of electric vehicle charging stations comprising multi-types of charging facilities, Applied energy 226 (2018) 1087–1099.

[17] B. Zhou, G. Chen, Q. Song, Z. Y. Dong, Robust chance-constrained programming approach for the planning of fast-charging stations in electrified transportation networks, Applied Energy 262 (2020) 114480.

[18] R. Gupta, A. Pena-Bello, K. N. Streicher, C. Roduner, D. Thöni, M. K. Patel, D. Parra, Spatial analysis of distribution grid capacity and costs to enable massive deployment of pv, electric mobility and electric heating, Applied Energy 287 (2021) 116504.

[19] R. Tu, Y. J. Gai, B. Farooq, D. Posen, M. Hatzopoulou, Electric vehicle charging optimization to minimize marginal greenhouse gas emissions from power generation, Applied Energy 277 (2020) 115517.

[20] M. R. Islam, H. Lu, M. J. Hossain, L. Li, Optimal coordination of electric vehicles and distributed generators for voltage unbalance and neutral current compensation, IEEE Transactions on Industry Applications 57 (1) (2020) 1069–1080.

[21] A. Zahedmanesh, K. M. Muttaqi, D. Sutanto, Coordinated charging control of electric vehicles while improving power quality in power grids using a hierarchical decision-making approach, IEEE Transactions on Vehicular Technology 69 (11) (2020) 12585–12596.

[22] Z. Liu, Q. Wu, K. Ma, M. Shahidehpour, Y. Xue, S. Huang, Two-stage optimal scheduling of electric vehicle charging based on transactive control, IEEE Transactions on Smart Grid 10 (3) (2019) 2948–2958.

[23] S. Xie, Z. Hu, J. Wang, Two-stage robust optimization for expansion planning of active distribution systems coupled with urban transportation networks, Applied Energy 261 (2020) 114412.

[24] T. Yang, Q. Guo, L. Xu, H. Sun, Dynamic pricing for integrated energy-traffic systems from a cyber-physical-human perspective, Renewable and Sustainable Energy Reviews 136 (2021) 110419.

[25] H. Wang, Y.-P. Fang, E. Zio, Risk assessment of an electrical power system considering the influence of traffic congestion on a hypothetical scenario of electrified transportation system in new york state, IEEE Transactions on Intelligent Transportation Systems 22 (1) (2021) 142–155.

[26] M. Shin, D.-H. Choi, J. Kim, Cooperative management for pv/ess-enabled electric vehicle charging stations: A multiagent deep reinforcement learning approach, IEEE Transactions on Industrial Informatics 16 (5) (2019) 3493–3503.

[27] H. Zhang, Z. Hu, Y. Song, Power and transport nexus: Routing electric vehicles to promote renewable power integration, IEEE Transactions on Smart Grid 11 (4) (2020) 3291–3301.

[28] W. Wei, L. Wu, J. Wang, S. Mei, Network equilibrium of coupled transportation and power distribution systems, IEEE Transactions on Smart Grid 9 (6) (2018) 6764–6779.

[29] X. Wang, M. Shahidehpour, C. Jiang, Z. Li, Coordinated planning strategy for electric vehicle charging stations and coupled traffic-electric networks, IEEE Transactions on Power Systems 34 (1) (2018) 268–279.

[30] L. Geng, Z. Lu, L. He, J. Zhang, X. Li, X. Guo, Smart charging management system for electric vehicles in coupled transportation and power distribution systems, Energy 189 (2019) 116275.

[31] S. Xie, Z. Hu, J. Wang, Y. Chen, The optimal planning of smart multi-energy systems incorporating transportation, natural gas and active distribution networks, Applied Energy 269 (2020) 115006.

[32] Z. Zhou, X. Zhang, Q. Guo, H. Sun, Analyzing power and dynamic traffic flows in coupled power and transportation networks, Renewable and Sustainable Energy Reviews 135 (2021) 110083.

[33] F. Rossi, R. Iglesias, M. Alizadeh, M. Pavone, On the interaction between autonomous mobility-on-demand systems and the power network:

Models and coordination algorithms, IEEE Transactions on Control of Network Systems 7 (1) (2019) 384–397.

[34] S. Lv, Z. Wei, G. Sun, S. Chen, H. Zang, Optimal power and semi-dynamic traffic flow in urban electrified transportation networks, IEEE Transactions on Smart Grid 11 (3) (2019) 1854–1865.

[35] S. Lv, Z. Wei, S. Chen, G. Sun, D. Wang, Integrated demand response for congestion alleviation in coupled power and transportation networks, Applied Energy 283 (2021) 116206.

[36] G. Sun, G. Li, S. Xia, M. Shahidehpour, X. Lu, K. W. Chan, Aladin-based coordinated operation of power distribution and traffic networks with electric vehicles, IEEE Transactions on Industry Applications 56 (5) (2020) 5944–5954.

[37] I. Yperman, The link transmission model for dynamic network loading.

[38] J. Long, W. Y. Szeto, Link-based system optimum dynamic traffic assignment problems in general networks, Operations Research 67 (1) (2019) 167–182.

[39] F. He, Y. Yin, S. Lawphongpanich, Network equilibrium models with battery electric vehicles, Transportation Research Part B: Methodological 67 (2014) 306–319.

[40] H. Wang, A. F. Abdin, Y.-P. Fang, E. Zio, Supplementary material, `https://github.com/lucky105/Coordinating-dynamic-traffic-power-systems-under-decentralized-centralized-and-formation-sharing`, accessed April. 2, 2021 (2021).